

ROM2F/2003/9

May 2003

Contributed paper to X International Workshop  
on "Neutrino Telescopes", Venice 2003**DAMA RESULTS**R. BERNABEI, P. BELLI, F. CAPPELLA, R. CERULLI, F. MONTECCHIA<sup>a</sup>, F. NOZZOLI*Dip. di Fisica, Universita' di Roma "Tor Vergata"  
and INFN, sez. Roma2, I-00133 Rome, Italy*

A. INCICCHITTI, D. PROSPERI

*Dip. di Fisica, Universita' di Roma "La Sapienza"  
and INFN, sez. Roma, I-00185 Rome, Italy*

and

C.J. DAI, H.H. KUANG, J.M. MA, Z.P. YE<sup>b</sup>*IHEP, Chinese Academy, P.O. Box 918/3, Beijing 100039, China***ABSTRACT**

DAMA is an observatory for rare processes based on the development and use of various kinds of radiopure scintillators. Several low background set-ups have been realized with time passing and many rare processes have been investigated. Main activities are briefly summarized in the following and the main arguments on the the results achieved in the investigation of the WIMP annual modulation signature are addressed. Next perspectives are also mentioned.

**1. Introduction**

DAMA is an observatory for rare processes based on the development and use of various kinds of radiopure scintillators. The main experimental set-ups are: i) the  $\simeq 100$  kg NaI(Tl) set-up, which has completed its data taking in July 2002; ii) the new 250 kg NaI(Tl) LIBRA (Large sodium Iodide Bulk for RAre processes) set-up, whose installation is started at fall 2002; iii) the  $\simeq 6.5$  kg liquid Xenon (LXe) pure scintillator; iv) the R&D installation for tests on prototypes and small scale experiments. Moreover, in the framework of devoted R&D for higher radiopure detectors and PMTs, sample measurements are regularly carried out by means of the low background DAMA/Ge detector, installed deep underground since about a decade and, in some cases, at Ispra.

The locations of the DAMA experimental installations in the Gran Sasso underground laboratory of I.N.F.N. are shown in Fig. 1.

---

<sup>a</sup>also: Universita' "Campus Biomedico" di Roma, 00155, Rome, Italy

<sup>b</sup>also: University of Zhao Qing, Guang Dong, China

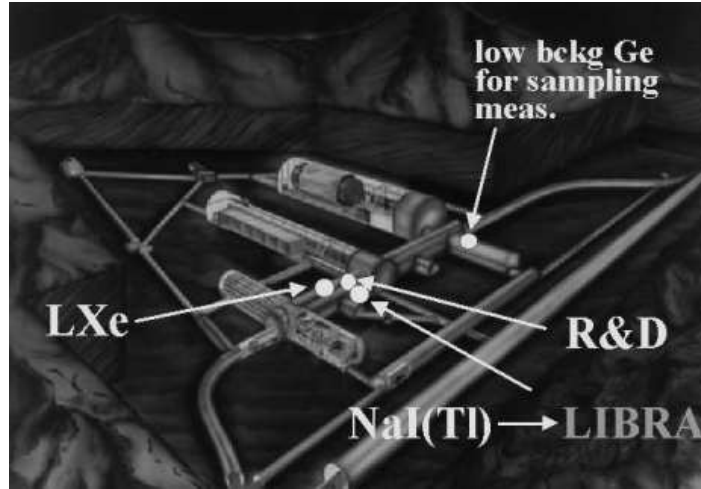


Figure 1: The locations of the DAMA experimental installations in the Gran Sasso underground laboratory of I.N.F.N.

## 2. DAMA/LXe

The DAMA/LXe experiment has followed the former Xelidon experiment on R&D developments of liquid Xenon (LXe) detectors and has realized since '90 several LXe scintillator prototypes using natural Xenon. Then, it has preliminarily put in measurement the set-up used in the data taking of ref. <sup>1,2)</sup> by using Kr-free Xenon enriched in  $^{129}\text{Xe}$  at 99.5%. This set-up was significantly upgraded at fall 1995 (as mentioned e.g. in ref. <sup>3)</sup>) by including: i) a new purification system without Oxisorb; ii) a new low background Pb in the shield; iii) a new low background Cu in the shield and in the insulation vessel; iv) a substitution of some PMTs and improved low background voltage dividers, etc. As a consequence, a significant improvement in the counting rate (as typically experienced in low background experiments; see e.g. the case of ref. <sup>4)</sup> for Ge detector) was obtained. The rate measured after this upgrading was well consistent over the whole energy spectrum and during several years of data taking, although some other minor substitutions have obviously been carried out with time passing.

In summer 2000 the set-up was again deeply modified (reaching the configuration reported in Fig.5 of ref. <sup>5)</sup>) to handle also Kr-free Xenon enriched in  $^{136}\text{Xe}$  at 68.8% and in  $^{134}\text{Xe}$  at 17.1% <sup>6,7)</sup>. The main differences among the previous and the present experimental set-up operating with this latter gas are: the gas<sup>c</sup>, part of the set-up<sup>d</sup>

<sup>c</sup>It was produced by another factory and many years before than the one enriched in  $^{129}\text{Xe}$ ; in addition, it was also previously used in a different underground experiment where different materials and vacuum/purification/filling/recovery system were operative and, afterwards, stored underground for long time in bottles with different possible effects from surface degassing, etc.; thus, the background is significantly different.

<sup>d</sup>The vacuum/purification/filling/recovery system has been significantly modified to allow the

and the isotope<sup>e</sup>. In particular, the high energy rate measured with this new set-up has been found higher than the one previously measured with the  $^{129}\text{Xe}$  set-up.

The main features of the set-up (see Fig. 2) are described in ref. <sup>5)</sup> and in related papers. We also remind that careful neutron calibrations have been carried out during

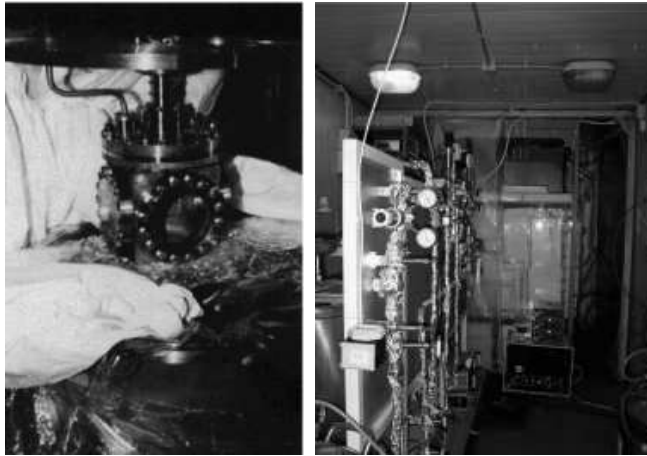


Figure 2: On the left: the vessel of the LXe set-up. On the right: the vacuum/purification/filling/recovery system and the passive shield ahead.

several years <sup>8,9)</sup>.

As regards the more recent results achieved with this set-up on the Dark Matter investigation we mention the limits on recoils obtained by investigating the WIMP- $^{129}\text{Xe}$  elastic scattering exploiting the pulse shape discrimination technique <sup>8)</sup> and those obtained – in a given model framework – on the WIMP- $^{129}\text{Xe}$  inelastic scattering <sup>3,10)</sup>.

The same experiment has allowed to investigate several other rare processes such as nuclear level excitation of  $^{129}\text{Xe}$  during charge-non-conserving processes <sup>11)</sup> and the possible electron decay through the channel:  $e^- \rightarrow \nu_e + \gamma$  <sup>12)</sup>. In addition, the nucleon and di-nucleon decay into invisible channels has been investigated with a new approach <sup>13)</sup> based on the search for the radioactive daughter nuclei, created after the nucleon or di-nucleon disappearance in the parent nuclei. The advantage of this approach is a branching ratio close to 1 and an efficiency – since the parent and the daughter nuclei are located in the detector itself – also close to 1. Competitive limits have been obtained.

After the latest upgrading of the set-up double beta decay modes in  $^{136}\text{Xe}$  and in  $^{134}\text{Xe}$  have been deeply investigated reaching competitive limits as well <sup>6,7)</sup>.

---

allocation and handling of the Xenon enriched in  $^{136}\text{Xe}$  and in some other parts such as the cold trap (a new concept one) and the shield.

<sup>e</sup>It can also be interested by different physical processes than the  $^{129}\text{Xe}$  previously used.

The data taking is continuing.

### 3. DAMA/R&D

The set-up named "R&D" is used for tests on prototypes and small scale experiments. A view of the passive shield of this installation is given in Fig. 3.

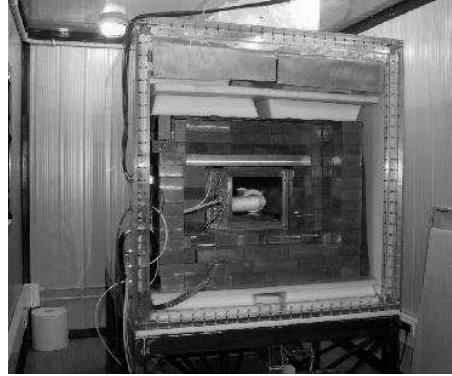


Figure 3: View of the open shield of the R&D installation.

This set-up which has been deeply upgraded in 2000/2001 has been used for measurements on low background prototype scintillators and PMTs realized in various R&D efforts with industries. Moreover, it is regularly used to perform small scale experiments mainly investigating double beta decay modes in various isotopes. Among the obtained results we remind the search for: i)  $\beta\beta$  decay modes in  $^{136}\text{Ce}$  and in  $^{142}\text{Ce}$  14); ii)  $2EC2\nu$  decay mode in  $^{40}\text{Ca}$  15); iii)  $\beta\beta$  decay modes in  $^{46}\text{Ca}$  and in  $^{40}\text{Ca}$  16); iv)  $\beta\beta$  decay modes in  $^{106}\text{Cd}$  17); v)  $\beta\beta$  and  $\beta$  decay modes in  $^{48}\text{Ca}$  18); vi)  $2EC2\nu$  in  $^{136}\text{Ce}$  and in  $^{138}\text{Ce}$  and  $\alpha$  decay in  $^{142}\text{Ce}$  19).

Fig. 4 summarizes the results obtained in the searches for double beta decay modes.

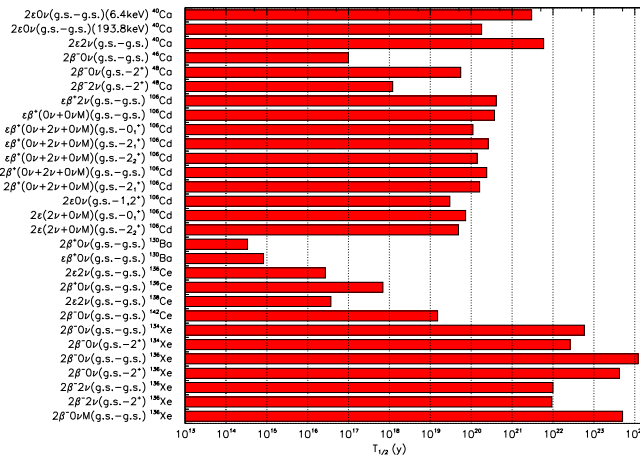


Figure 4: Summary of the limits obtained by DAMA on various double beta decay processes. See text.

#### 4. DAMA/Ge for sampling measurements

Various R&D developments to improve low background set-ups and scintillators as well as new developments for higher radiopure PMTs are regularly carried out. The related measurements on samples are performed by means of the DAMA low background Ge detector<sup>f</sup>, which is operative deep underground in the low background facility of the Gran Sasso National Laboratory since many years.

#### 5. DAMA/NaI

The main goal of the  $\simeq 100$  kg NaI(Tl) (DAMA/NaI) set-up has been the search for WIMPs by the annual modulation signature, which it has investigated over seven annual cycles; the data of 4 of them (about 60000 kg·d) have been already released (20,21,22,23,24,25,26,27,28) and main arguments will be discussed in the following.

For completeness, we remind that – in addition to the investigation of the WIMP component in the galactic halo by means of the annual modulation signature – other approaches have also been exploited with DAMA/NaI such as the pulse shape discrimination technique<sup>29)</sup> and the investigation of possible diurnal effects<sup>30)</sup>. Moreover, also exotic Dark Matter candidates such as neutral SIMPs, neutral nuclearities and Q-balls<sup>31,32)</sup> have been searched for. A devoted search for solar axions has been carried out as well (see Fig. 5)<sup>33)</sup>.

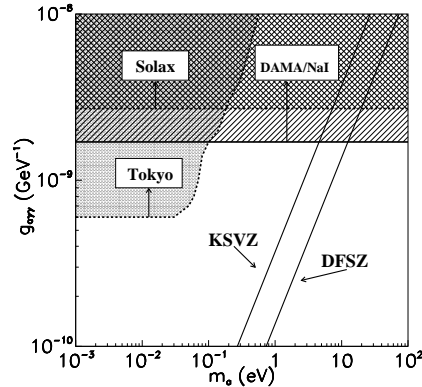


Figure 5: Exclusion plot in the plane axion to photon coupling constant,  $g_{a\gamma\gamma}$ , versus axion mass,  $m_a$ , achieved by DAMA/NaI in ref. <sup>33)</sup>. The limit quoted in the paper ( $g_{a\gamma\gamma} \leq 1.7 \times 10^{-9} \text{GeV}^{-1}$  at 90% C.L.) is shown together with the expectations of the KSVZ and DFSZ models; see ref. <sup>33)</sup> for details.

In addition, DAMA/NaI has also allowed to investigate several other rare processes such as e.g. Pauli exclusion principle violation with spontaneous emission of protons

<sup>f</sup>This detector was specially realized with a low Z window to be sensitive to external radiation down to about ten keV.

in  $^{23}\text{Na}$  and  $^{127}\text{I}$  <sup>34)</sup>, nuclear level excitation of  $^{127}\text{I}$  and  $^{23}\text{Na}$  during charge-non-conserving processes <sup>35)</sup> and electron stability and non-paulian transitions in Iodine atoms (by L-shell) <sup>36)</sup>.

The set-up and its performances have been described in details in ref. <sup>21)</sup>; since then some upgrading has been carried out. In particular, in summer 2000 the electronic chain and data acquisition system have been completely substituted, while during August 2001 the new HV power supply system and the new preamplifiers prepared for the foregoing LIBRA set-up have been installed here.

The set-up has completed its data taking in July 2002. Various kind of data analyses are continuing; in particular, the total statistics of 107731 kg·d will be presented in near future giving further results on the WIMP annual modulation signature.

### *5.1. Results on the WIMP annual modulation signature*

DAMA/NaI has been proposed in '90 <sup>37)</sup> and has been realized to investigate with suitable sensitivity the WIMP annual modulation signature, originally proposed in ref. <sup>38)</sup>. It has been so far the only experiment able to test this model independent signature for WIMPs with suitable mass, sensitivity and control of the running parameters.

This WIMP model independent signature is based on the annual modulation of the signal rate induced by the Earth revolution around the Sun; as a consequence, the Earth will be crossed by a larger WIMP flux roughly in June (when its rotational velocity is summed to the one of the solar system with respect to the Galaxy) and by a smaller one roughly in December (when the two velocities are subtracted). The fractional difference between the maximum and the minimum of the rate is of order of  $\simeq 7\%$ . Therefore, to point out the modulated component of the signal, large mass apparatus with suitable performances and control of the operating conditions – such as the  $\simeq 100$  kg highly radiopure NaI(Tl) DAMA set-up – are necessary.

The annual modulation signature is very distinctive since a WIMP-induced seasonal effect must simultaneously satisfy all the following requirements: the rate must contain a component modulated according to a cosine function (1) with one year period (2) and a phase that peaks around  $\simeq 2^{\text{nd}}$  June (3); this modulation must only be found in a well-defined low energy range, where WIMP induced recoils can be present (4); it must apply to those events in which just one detector of many actually "fires", since the WIMP multi-scattering probability is negligible (5); the modulation amplitude in the region of maximal sensitivity must be  $\lesssim 7\%$  (6). Only systematic effects able to fulfil these 6 requirements could fake this signature; no one has been

found nor suggested by anyone after several years of investigations.

### 5.1.1. The model independent evidence by DAMA/NaI

A model independent analysis of the data of the four annual cycles has offered an immediate evidence of the presence of an annual modulation of the rate of the single hit events in the lowest energy interval (2 – 6 keV) as shown in Fig. 6. The  $\chi^2$  test on

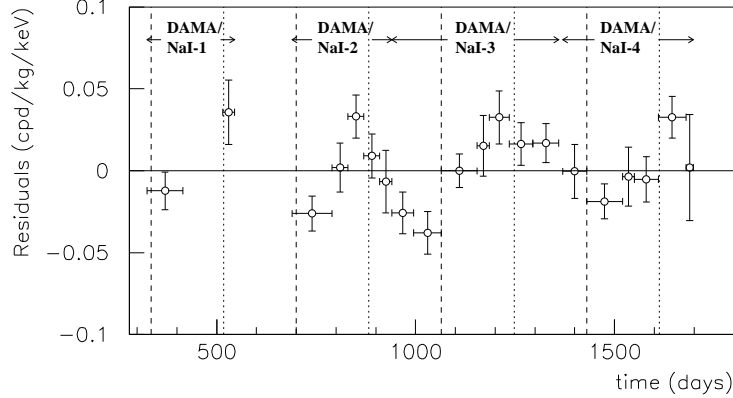


Figure 6: Model independent residual rate for single hit events, in the 2–6 keV cumulative energy interval, as a function of the time elapsed since January 1-st of the first year of data taking. The expected behaviour of a WIMP signal is a cosine function with minimum roughly at the dashed vertical lines and with maximum roughly at the dotted ones.

the data of Fig. 6 disfavors the hypothesis of unmodulated behaviour (probability:  $4 \cdot 10^{-4}$ ), while fitting these residuals with the function  $A \cdot \cos\omega(t - t_0)$ , one gets: i) for the period  $T = \frac{2\pi}{\omega} = (1.00 \pm 0.01)$  year when  $t_0$  is fixed at the 152.5<sup>th</sup> day of the year (corresponding to  $\simeq 2$  June); ii) for the phase  $t_0 = (144 \pm 13)$  days, when  $T$  is fixed at 1 year. In the two cases  $A$  is:  $(0.022 \pm 0.005)$  cpd/kg/keV and  $(0.023 \pm 0.005)$  cpd/kg/keV, respectively. Similar results, but with slightly larger errors, are found in case all the parameters are kept free.

The modulation is absent in other part of the energy spectrum as discussed e.g. in ref. <sup>25)</sup>; for example, in the 6-10 keV energy region just above a modulation amplitude  $A = -(0.0017 \pm 0.0037)$  cpd/kg/keV is obtained.

We have extensively discussed the results of the investigations of all sources of possible systematics when releasing the data of each annual cycle; moreover, a dedicated paper <sup>25)</sup> has been devoted to this subject. No systematic effect or side reaction able to mimic a WIMP induced effect (that is to be both quantitative relevant and able to satisfy the six peculiarities of the WIMP signature) has been found. This deep discussion will not be repeated here since the reader can directly find it in ref. <sup>25)</sup> with all the details.

In conclusion, a WIMP contribution to the measured rate has been candidate by the result of the model independent approach independently on the nature and

coupling with ordinary matter of the involved WIMP particle. This is the main experimental result of DAMA/NaI.

No other experiment has been realized so far able to exploit this model independent approach with similar exposed mass, sensitivity and control of the running parameters as DAMA/NaI.

### 5.1.2. The corollary model dependent analyses searching for the nature of a candidate

A corollary investigation can be pursued to investigate the nature and coupling with ordinary matter of a possible candidate. In this case, a suitable energy and time correlation analysis is necessary as well as the choice of a complete model framework. We remark that a model framework is identified not only by the general astrophysical, nuclear and particle physics assumptions, but also by the set of values used for all the experimental and theoretical parameters needed in the calculations (for example WIMP local velocity,  $v_0$ , form factors and related parameters, quenching factors, halo model, coupling, etc., which are affected by relevant uncertainties) <sup>8</sup>.

For simplicity, initially we have considered the particular case of purely spin-independent (SI) coupled WIMP. In fact, often the spin-independent interaction with ordinary matter is assumed to be dominant since e.g. most of the used target-nuclei are practically not sensitive to SD interactions as on the contrary  $^{23}\text{Na}$  and  $^{127}\text{I}$  are and the theoretical calculations are even more complex when including also this latter kind of interaction. Moreover, only one set of possible parameters values has been adopted <sup>20,22</sup>). Then, this case has been extended by considering some of the existing uncertainties on the astrophysical velocity distribution <sup>23,24</sup>) and the physical constraint which arises from the upper limits on recoils measured by the same set-up <sup>24</sup>). More recently an investigation on the effect induced on the result by considering other possible and consistent halo models still for the particular case of purely SI coupled WIMPs has also been carried out in ref. <sup>28</sup>).

Moreover, some of the other possible scenarios have also been considered such as extensions to the general case of WIMPs with both spin-independent (SI) and spin-dependent (SD) coupling <sup>26</sup>) and to the case of WIMPs with preferred inelastic scattering <sup>27</sup>). In these latter cases, the effect of the uncertainties on some of the parameters has been included, but still only the simplified, approximate and non-consistent isothermal halo model has been considered in the calculations.

Theoretical implications in terms of a neutralino with dominant SI interaction have been discussed e.g. in ref. <sup>42,43</sup>) for some theoretical model frameworks and in terms of an heavy neutrino of the fourth family in ref. <sup>44</sup>).

---

<sup>8</sup>Note that results given in terms of exclusion plots by experiments such as <sup>39,40,41</sup>) also depend on their own choice of nuclear, particle and astrophysical assumptions and of experimental/theoretical parameters values; thus they have no generality at all.

### 5.1.2.1 WIMPs with dominant SI interaction in given model frameworks

A full energy and time correlation analysis – properly accounting for the physical constraint arising from the measured upper limit on recoils <sup>25,29)</sup> – has been carried out in the framework of given model for purely spin-independent coupled candidates with mass above 30 GeV (this bound being inspired by the lower bound on the supersymmetric candidate, as derived from the LEP data in the usually adopted supersymmetric schemes based on GUT unification assumptions). A standard maximum likelihood method has been used. Note that different model frameworks (see above) vary the theoretical expectations and, therefore, the best fit values of cross section and mass (as well as the allowed region) also vary. In particular, the inclusion of the uncertainties associated to the models and to every parameter in the models themselves as well as other possible scenarios largely enlarges the allowed region as discussed e.g. in ref. <sup>23)</sup> for the particular case of the astrophysical velocities and offers very large sets of best fit values. We take this occasion to stress that ref. <sup>24)</sup> also accounts for several models; thus, for several sets of best fit values <sup>h</sup>. Therefore, claims for contradiction in model dependent comparisons by ”choosing” a particular set of best fit values, given there as an example, are – also in this respect – arbitrary and substantially wrong.

As mentioned, more recently possible departures from the isothermal sphere model, which is the parameterisation usually adopted only in direct WIMP searches to describe the halo although approximate and non-consistent, have been investigated in a systematic way in ref. <sup>28)</sup> by some of us in collaboration with N. Fornengo and S. Scopel. Modifications arising from various matter density profiles, effects due to anisotropies of the velocity dispersion tensor and rotation of the galactic halo have been specifically investigated. In particular, several halo models with potential and matter density having a spherical symmetry have been investigated as well as halo models with spherical symmetry but anisotropic WIMP velocity distribution and halo models with axial symmetry (in these latter cases possible co-rotation or counter-rotation of the dark halo has also been considered). Also some triaxial models have been investigated.

The global results of this analysis – which includes also those presented in ref. <sup>24)</sup> – are shown in Fig. 7, where the allowed regions obtained for the various considered halo models in given framework for three of the possible values of the local velocity,  $v_0$ , above WIMP mass of 30 GeV are superimposed. Obviously different best fit values correspond to each one. The cumulative result, which gives a direct impact of the

---

<sup>h</sup>For example, for the particular model frameworks and assumptions of ref. <sup>24)</sup>, where the WIMP local velocity,  $v_0$ , has been varied from 170 km/s to 270 km/s to account for its present uncertainty, we obtained the best fit values  $m_W = (72_{-15}^{+18})$  GeV and  $\xi\sigma_{SI} = (5.7 \pm 1.1) \cdot 10^{-6}$  pb for  $v_0 = 170$  km/s and  $m_W = (43_{-9}^{+12})$  GeV and  $\xi\sigma_{SI} = (5.4 \pm 1.0) \cdot 10^{-6}$  pb for  $v_0 = 220$  km/s. Here,  $\xi$  is the WIMP local density in  $0.3 \text{ GeV cm}^{-3}$  unit,  $\sigma_{SI}$  is the point-like SI WIMP-nucleon generalized cross section and  $m_W$  is the WIMP mass.

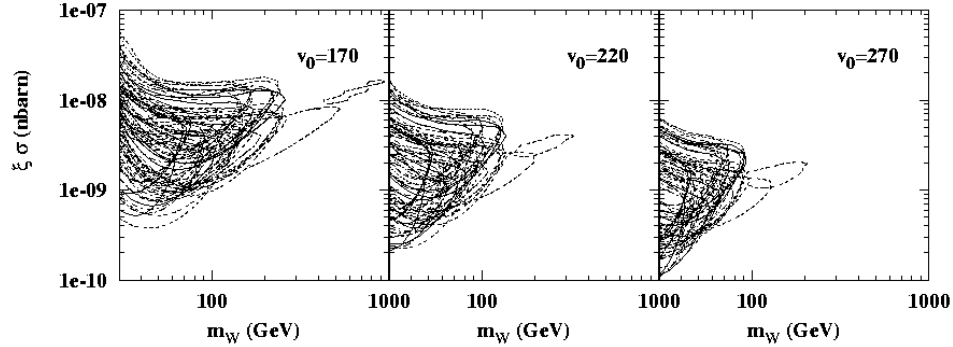


Figure 7: Superposition of the regions allowed at  $3\sigma$  C.L. in the given model frameworks by considering the velocity distribution of each one of the halo models in ref. <sup>28)</sup>. Three of the possible values of  $v_0$  are considered. Obviously a specific set of best fit values for the WIMP mass and cross section corresponds to each region. Note that inclusion of other existing uncertainties will further enlarge the regions and increase the sets of best fit values.

effect induced on the region allowed in the considered scenario only by the present poor knowledge of the right halo model, is shown in Fig. 8. This region is compared with

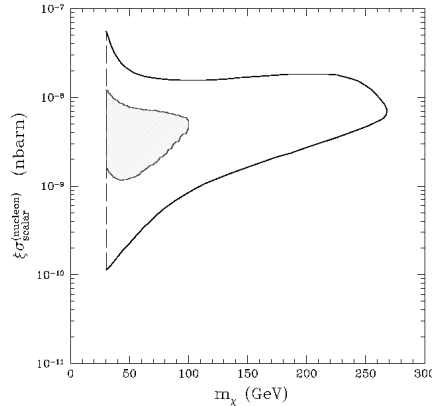


Figure 8: Region allowed at  $3\sigma$  C.L. given by the superposition of all the allowed regions obtained, in the given model frameworks, considering several possible non-rotating halo models <sup>28)</sup>. Note that in these calculations only uncertainties on the halo model have been considered; the inclusion of the other existing uncertainties would further enlarge it. It is evident that this cumulative region, as those given e.g. in ref. <sup>23,24)</sup>, accounts for a large set of best fit values for WIMP mass and cross section. The shaded region (which corresponds to the particular case of the approximate and non-consistent isothermal sphere halo model when assuming also  $v_0 = 220$  km/s and  $\rho_0 = 0.3$  GeV/cm<sup>3</sup> for the astrophysical, nuclear and particle physics assumptions and fixed parameters of ref. <sup>28)</sup>) is shown to point out only the effect due to the poor knowledge of the right halo model.

the one obtained when considering, for a particular model framework (of the many possible), the approximate and non-consistent isothermal sphere halo model assuming

in particular also  $v_0 = 220 \text{ km/s}$  e  $\rho_0 = 0.3 \text{ GeV/cm}^3$ . As one can see, the cumulative  $3 \sigma$  C.L. allowed region is extended up to  $m_W \simeq 270 \text{ GeV}$  with cross section on nucleon in the range  $10^{-10} \text{ nbarn} \leq \xi\sigma_{SI} \leq 6 \cdot 10^{-8} \text{ nbarn}$ . Maximal co-rotating and counter-rotating models can extend the allowed region up to  $m_W \simeq 500 - 900 \text{ GeV}$  (see Fig. 7). We further stress that in this analysis no other uncertainty than the halo model <sup>i</sup> has been considered; the proper inclusion of the other existing uncertainties will further extend the cumulative allowed region and offer further sets of best fit values. In particular, as already stressed also e.g. in ref. <sup>24)</sup>, in all the analyses cautiously the Helm SI form factor has been adopted, which is the most cautious one for Iodine. The use of other form factors enhancing the expected signal from Iodine recoils would yield allowed regions corresponding to lower cross section values. The same would be if a spin-dependent component different from zero would be introduced <sup>26)</sup> (see also next section).

### 5.1.2.2 WIMPs with mixed coupling in given model frameworks

Since the  $^{23}\text{Na}$  and  $^{127}\text{I}$  nuclei are sensitive to both SI and SD couplings – on the contrary e.g. of  $^{nat}\text{Ge}$  and  $^{nat}\text{Si}$  which are sensitive mainly to WIMPs with SI coupling (only 7.8 % is non-zero spin isotope in  $^{nat}\text{Ge}$  and only 4.7% of  $^{29}\text{Si}$  in  $^{nat}\text{Si}$ ) – the analysis of the data has been extended considering the more general case of a WIMP having not only a spin-independent, but also a spin-dependent coupling different from zero <sup>j</sup>.

In this case the free parameters are  $\xi\sigma_{SI}$ ,  $\xi\sigma_{SD}$  and  $m_W$  for each given  $\theta$  value, where  $\sigma_{SD}$  is the point-like SD WIMP cross section on nucleon and  $tg\theta$  is the ratio between the effective SD coupling constants on neutrons,  $a_n$ , and on proton,  $a_p$ ; therefore,  $\theta$  can assume all the values between 0 and  $\pi$  depending on the type of SD coupling.

Note that the results in ref. <sup>26)</sup> have been obtained by considering there only the approximate non-consistent isothermal sphere model to describe the galactic halo and a maxwellian WIMP velocity distribution with inclusion of some uncertainties on  $v_0$ , on the nuclear radius and on the nuclear surface thickness parameter in the used Helm SI form factor, on the  $b$  parameter in the used Ressel e al. SD

---

<sup>i</sup>We note that, although the large number of halo models considered in this analysis, many other halo models are still possible, available and not yet considered here.

<sup>j</sup>We take this occasion to note that on the contrary of what is reported on <sup>45)</sup>, ref. <sup>46)</sup> does not exclude at all a possible spin-dependent solution. In fact, it refers only to the two particular cases (of the many possible) for purely spin-dependent coupling: specifically the case where the effective coupling constant on proton is equal to zero and the case where the effective coupling constant on neutron is equal to zero. In addition, not only these two cases are handled in strongly model dependent mode, but are even based on the wrong use of modulation amplitudes calculated for a particular purely spin-independent case. Thus no restriction at all arises – by the fact – from ref. <sup>46)</sup> for any possible purely SD solution. In addition, the mixed case was not involved at all in that discussion.

form factor and on the quenching factors. As an additional source of uncertainty we mention that an universal formulation is not possible for the SD form factor, thus other formulations than the one adopted here are possible and can be considered with evident implications on the obtained results. The same is for the used spin factor.

For simplicity, Fig. 9 shows slices for some  $m_W$  of the region allowed – in the model frameworks of ref. 26) – at  $3\sigma$  C.L. in the  $(\xi\sigma_{SI}, \xi\sigma_{SD}, m_W)$  space for four particular couplings: i)  $\theta = 0$  ( $a_n = 0$  and  $a_p \neq 0$  or  $|a_p| \gg |a_n|$ ); ii)  $\theta = \pi/4$  ( $a_p = a_n$ ); iii)  $\theta = \pi/2$  ( $a_n \neq 0$  and  $a_p = 0$  or  $|a_n| \gg |a_p|$ ); iv)  $\theta = 2.435$  rad ( $\frac{a_n}{a_p} = -0.85$ , pure  $Z^0$  coupling). The case  $a_p = -a_n$  is nearly similar to the case iv).

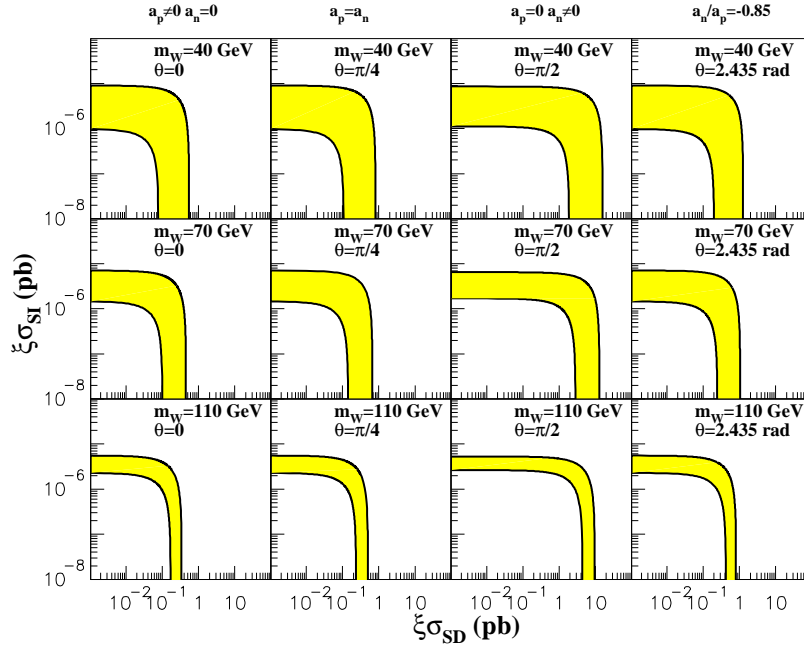


Figure 9: A mixed SI/SD case: example of slices of the region allowed at  $3\sigma$  C.L. in the  $(\xi\sigma_{SI}, \xi\sigma_{SD}, m_W)$  space for some  $m_W$  and  $\theta$  values in the model frameworks considered in ref. 26). Only four particular couplings are reported here for simplicity: i)  $\theta = 0$ ; ii)  $\theta = \pi/4$  iii)  $\theta = \pi/2$ ; iv)  $\theta = 2.435$  rad. Note that e.g. Ge experiments are sensitive mainly only to SI coupling and, therefore, cannot explore most of the DAMA allowed regions in this scenario; the same is in most cases also for  $^{nat}\text{Xe}$  since the odd-spin isotopes have the neutron as unpaired nucleon. These allowed regions would be further enlarged by taking into account the uncertainties existing on the halo models and related parameters, on the SD form factor (which has a not an universal formulation) and on some other experimental and theoretical parameters and assumptions.

As already pointed out, when the SD contribution goes to zero (y axis in Fig. 9), an interval not compatible with zero is obtained for  $\xi\sigma_{SI}$ . Similarly, when the SI contribution goes to zero (x axis in Fig. 9), finite values for the SD cross section are obtained. Large regions are allowed for mixed configurations in the considered model frameworks also for  $\xi\sigma_{SI} \lesssim 10^{-5}$  pb and  $\xi\sigma_{SD} \lesssim 1$  pb; only in the particular case of  $\theta = \frac{\pi}{2}$  (that is  $a_p = 0$  and  $a_n \neq 0$ )  $\xi\sigma_{SD}$  can increase up to  $\simeq 10$  pb, since the  $^{23}\text{Na}$

and  $^{127}\text{I}$  nuclei have the proton as odd nucleon. Moreover, in ref. <sup>26)</sup> we have also pointed out that: i) finite values can be allowed for  $\xi\sigma_{SD}$  even when  $\xi\sigma_{SI} \simeq 3 \cdot 10^{-6}$  pb as in the region allowed in the pure SI scenarios considered above; ii) regions not compatible with zero in the  $\xi\sigma_{SD}$  versus  $m_W$  plane are allowed even when  $\xi\sigma_{SI}$  values much lower than those allowed in the dominant SI scenarios previously summarized are considered; iii) best fit values with both  $\xi\sigma_{SI}$  and  $\xi\sigma_{SD}$  different from zero are present for some  $m_W$  and  $\theta$  pairs; the related confidence level ranges between  $\simeq 3 \sigma$  and  $\simeq 4 \sigma$  <sup>26)</sup>.

Further investigations are in progress on these model dependent analyses to account for other known parameters uncertainties and for possible different model assumptions. In fact, as mentioned, when including the uncertainties on the halo models and their parameters, on the SD form factor, on the spin factor and on some other experimental and theoretical parameters, the allowed volume in the space ( $\xi\sigma_{SI}$ ,  $\xi\sigma_{SD}$ ,  $m_W$ ) for each  $\theta$  value would be further enlarged as well as the number of obtained sets of best fit values for the cross sections and the WIMP mass.

In conclusion, this analysis has shown that the DAMA data of the four annual cycles, analysed in terms of WIMP annual modulation signature, can also be compatible with a mixed scenario where both  $\xi\sigma_{SI}$  and  $\xi\sigma_{SD}$  are different from zero.

### 5.1.2.3 Inelastic Dark matter

It has been suggested in ref. <sup>47)</sup> that the observed annual modulation effect could be induced by possible inelastic Dark Matter: relic particles that prefer to scatter inelastically off of nuclei. The inelastic Dark Matter could arise from a massive complex scalar split into two approximately degenerate real scalars or from a Dirac fermion split into two approximately degenerate Majorana fermions, namely  $\chi_+$  and  $\chi_-$ , with a  $\delta$  mass splitting. In particular, a specific model featuring a real component of the sneutrino, in which the mass splitting naturally arises, has been given in ref. <sup>47)</sup>. It has been shown that for the  $\chi_-$  inelastic scattering on target nuclei a kinematical constraint exists which favours heavy nuclei (such as  $^{127}\text{I}$ ) with respect to lighter ones (such as e.g.  $^{nat}\text{Ge}$ ) as target-detectors media. In fact,  $\chi_-$  can only inelastically scatter by transitioning to  $\chi_+$  (slightly heavier state than  $\chi_-$ ) and this process can occur only if the  $\chi_-$  velocity is larger than  $v_{thr} = \sqrt{\frac{2\delta}{m_{WN}}}$  where  $m_{WN}$  is the WIMP-nucleus reduced mass ( $c = 1$ ). This kinematical constraint becomes increasingly severe as the nucleus mass,  $m_N$ , is decreased <sup>47)</sup>. Moreover, this model scenario gives rise – with respect to the case of WIMP elastically scattering – to an enhanced modulated component,  $S_m$ , with respect to the unmodulated one,  $S_0$ , and to largely different behaviours with energy for  $S_0$  and  $S_m$  (both show a higher mean value) <sup>47)</sup>.

A dedicated energy and time correlation analysis of the DAMA annual modulation data has been carried out <sup>27)</sup> handling aspects other than the interaction type as in ref. <sup>26)</sup>. In this scenario of Dark Matter with inelastic scattering an allowed volume in the space ( $\xi\sigma_p$ ,  $\delta$ ,  $m_W$ ) is obtained <sup>27)</sup>. For simplicity, Fig. 10 shows slices of

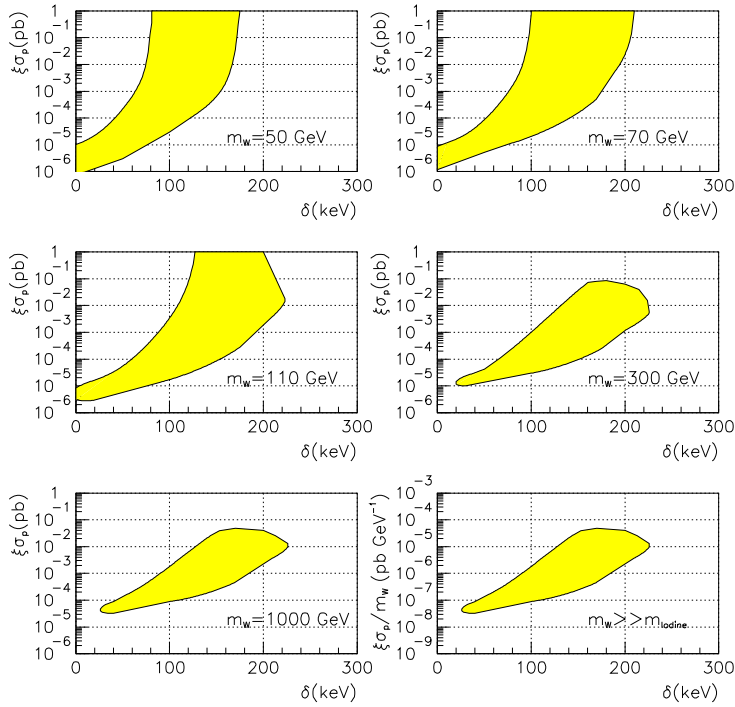


Figure 10: An inelastic case: slices at fixed WIMP masses of the volume allowed at  $3 \sigma$  C.L. in the space  $(\xi\sigma_p, \delta, m_W)$  obtained for the model frameworks considered in ref. <sup>27)</sup>; some of the uncertainties on used parameters have been included. Note that e.g. Ge experiments cannot explore most of the DAMA allowed regions in this scenario. These allowed regions would be further enlarged by taking into account the uncertainties existing on the halo models and their parameters and on some other experimental and theoretical parameters.

such an allowed volume at some given masses ( $3 \sigma$  C.L.) for the model frameworks considered in ref. <sup>27)</sup>. It can be noted that when  $m_W \gg m_N$ , the expected differential energy spectrum is trivially dependent on  $m_W$  and in particular it is proportional to the ratio between  $\xi\sigma_p$  and  $m_W$ ; this particular case is summarized in the last plot of Fig. 10. The allowed regions have been obtained – as in the previous cases – by the superposition of those obtained when varying the values of some of the used parameters according to ref. <sup>27)</sup>. Of course, each set of parameters’ values gives rise to a different expectation, thus to different ”most likely” values. Just as an example we mention that when fixing the other parameters as in ref. <sup>26)</sup>, the ”most likely” values for a WIMP mass of 70 GeV are: i)  $\xi\sigma_p = 2.5 \times 10^{-2}$  pb and  $\delta = 115$  keV when  $v_0 = 170$  km/s, ii)  $\xi\sigma_p = 6.3 \times 10^{-4}$  pb and  $\delta = 122$  keV when  $v_0 = 220$  km/s; they are in  $\delta$  region where e.g. Ge and Si experiments are disfavoured.

Finally, we note again that the allowed regions are further enlarged when properly including the uncertainties on the halo models, on the experimental and theoretical

parameters and on the other assumptions.

### 5.1.3. Comparison with some model dependent results

#### 5.1.3.1 ... from direct searches

As mentioned above no other experiment directly comparable with the model independent DAMA/NaI result on WIMPs in the galactic halo is available at present; thus, claims for contradiction are intrinsically arbitrary/wrong.

Only few experiments <sup>39,40,41)</sup>, which use different target nuclei and different methodological approaches, have released extremely poor selected statistics quoting an exclusion plot in a given particular model framework.

Table 1 shortly summarizes some main items. As it can be seen, the mentioned exclusion plots are based on a huge data selection (releasing typically extremely poor exposures with respect to generally long data taking and, in some cases, to several used detectors). Moreover, their counting rate is very high and few/zero events are claimed after applying several strong and hardly safe rejection procedures (involving several orders of magnitude; see Table 1). These rejection procedures are also poorly described and, often, not completely quantified. Moreover, most efficiencies and physical quantities entering in the interpretation of the claimed selected events have never been discussed in the needed details. As an example, we mention the case of the quenching factor of the recoil target nuclei in the whole bulk material for the bolometer cases, which is arbitrarily assumed to be 1 <sup>k</sup>, implying a substantially arbitrarily assumed energy scale and energy threshold (and consequently arbitrary exclusion plot). Further uncertainties are present when, as in ref. <sup>39)</sup>, a neutron background modeling and subtraction is pursued in addition.

As regards in particular the Zeplin-I result of ref. <sup>41,49)</sup>, a very low energy threshold is claimed (2 keV), although the light response is very poor: between  $\simeq 1$  ph.e./keV <sup>49)</sup> (for most of the time) and  $\simeq 2.5$  ph.e./keV (claimed for 16 days) <sup>41)</sup>. Moreover, a strong data filtering is applied to the high level of measured counting rate ( $\simeq 100$  cpd/kg/keV at low energy, which is nearly two orders of magnitude larger than the DAMA NaI(Tl) background in the same energy region) by hardware vetoes,

---

<sup>k</sup>In fact, no direct measurement performed with neutron sources or generators has been reported up to now, although several bolometers have been irradiated with neutrons along the past decade. For the sake of completeness, we remind that a measurement of the response of a TeO<sub>2</sub> bolometer to surface <sup>224</sup>Ra recoiling nuclei has been reported in ref. <sup>48)</sup>; this measurement, although its importance, does not represent a determination of the quenching factor for a bolometer since neither the target-nuclei nor the whole bulk of the detector are involved. Moreover, these values cannot of course be extended to whatever kind of bolometer.

<sup>l</sup>For comparison we remind that the data of the DAMA/LXe set-up, which has a similar light response, are analysed by using the much more realistic and safer software energy threshold of 13 keV <sup>8)</sup>.

Table 1: Features of the DAMA/NaI results on the WIMP annual modulation signature during the first four annual cycles (57986 kg  $\times$  day exposure) <sup>20,22,23,24,25,26,27,28</sup> and those of refs. <sup>39,40,41</sup>.

	DAMA/NaI	CDMS-I	Edelweiss-I	Zeplin-I
Signature	annual modulation	None	None	None
Target-nuclei	<sup>23</sup> Na, <sup>127</sup> I	<i>nat</i> Ge	<i>nat</i> Ge	<i>nat</i> Xe
Technique	well known	poorly experienced	poorly experienced	critical optical liquid/gas interface in this realization
Target mass	$\simeq 100$ kg	0.5 kg	0.32 kg	$\simeq 3$ kg
Exposure	57986 kg $\times$ day	15.8 kg $\times$ day	8.2 kg $\times$ day	280 kg $\times$ day
Depth of the experimental site	1400 m	10 m	1700 m	1100 m
Software energy threshold (electron equivalent)	2 keV (5.5 – 7.5 p.e./keV)	10 keV	20 keV	2 keV (but: $\sigma/E = 100\%$ mostly 1 p.e./keV; <sup>49</sup> ) (2.5 p.e./keV for 16 days; <sup>41</sup> )
Quenching factor	Measured	Assumed = 1	Assumed = 1	Measured
Measured event rate in low energy range	$\simeq 1$ cpd/kg/keV	$\simeq 60$ cpd/kg/keV ( $10^5$ events)	2500 events total	$\simeq 100$ cpd/kg/keV
Claimed events after rejection procedures		23 in Ge, 4 in Si, 4 multiple evts in Ge + MonteCarlo on neutron flux	0	$\simeq 20$ -50 cpd/kg/keV after rejection and ?? after standard PSD <sup>41,49</sup> )
Events satisfying the signature in DAMA/NaI	modulation amplitude integrated over the given exposure $\simeq 2000$ events			
Expected number of events from DAMA/NaI effect		from few down to zero depending on the models (and on quenching factor)	from few down to zero depending on the models (and on quenching factor)	depends on the models (even zero)

by fiducial volume cuts and, largely, by applying down to few keV a standard pulse shape discrimination procedure, although the LXe scintillation pulse profiles (pulse decay time  $< 30$  ns) are quite similar even to noise events in the lower energy bins and in spite of the poor light response. Quantitative information on experimental quantities related to the used procedures has not yet been given <sup>41,49</sup>).

In addition to the experimental aspects, these experiments – which cannot perform any model independent comparison with the result of DAMA/NaI – generally uncorrectly/partially quote the results of published quests for a purely SI coupled candidate in given model frameworks and ignore the effects of the relevant uncertainties in the astrophysical, nuclear and particle physics assumptions and experimental/theoretical parameters values taken by each experiments as well as the interpretation of the DAMA/NaI model independent effect in terms of candidates with other kind of coupling. All that can significantly vary the result of any comparison (even when assuming as correct the evaluation of the selected number of events, the energy scale and the energy threshold determinations given in refs. <sup>39,40,41,49</sup>) and the used efficiencies, etc.). In addition, there exist scenarios to which Na and I are sensitive and other nuclei, such as e.g.  $^{nat}\text{Ge}$ ,  $^{nat}\text{Si}$  and  $^{nat}\text{Xe}$ , are not.

In conclusion:

1. no other experiment, whose result can be directly comparable in a model independent way with that of DAMA/NaI, is available so far.
2. as regards in particular CDMS-I, EDELWEISS-I and Zeplin-I, e.g.:
  - i) they are insensitive to the model independent WIMP annual modulation signature exploited by DAMA/NaI; ii) they use different methodological approaches, which do not allow any model independent comparison and they have different sensitivities to WIMPs; in particular, the number of counts they could expect on the basis of the model independent DAMA/NaI result varies from few to zero events depending on the models, on the assumptions and on the theoretical/experimental parameters' values adopted in the calculations; iii) they make neither correct nor complete comparisons with the DAMA/NaI experimental result; iv) they use extremely poor statistics; v) they reduce their huge measured counting rate of orders of magnitude by various rejection procedures claiming for very optimistic rejection powers; vi) their energy scale determination and/or energy threshold appear questionable (in the first two cases because of the quenching factors values and in the second because of the poor number of photoelectrons/keV); etc.

### 5.1.3.2 ... from indirect searches

As regards results from indirect searches, model dependent analyses investigating possible up-going muons arising from WIMP annihilation in celestial bodies have been carried out by large experiments deep underground such as e.g. Macro and Superkamiokande. The comparison is strongly model dependent; anyhow it has already been shown in ref. <sup>42</sup>) that even in the simple model frameworks considered in ref. <sup>24</sup>) the model dependent limit on up-going muon flux obtained by Macro (and thus that by Superkamiokande, which is only slightly more stringent) could cut only part of the allowed configurations in MSSM.

On the other hand, as regards antimatter searches carried out outside the atmosphere, we remind the analysis of the HEAT balloon-borne experiment performed in ref. <sup>50)</sup>, where an excess of positrons with energy  $\simeq 5 - 20$  GeV has been found and has been interpreted in terms of WIMP annihilation. We also mention the analysis of ref. <sup>51)</sup> which already suggests the presence of a  $\gamma$  excess from the center of the Galaxy in the EGRET data <sup>52)</sup> which matches with a possible WIMP annihilation in the galactic halo and is not in conflict with the DAMA/NaI model independent result.

We take this occasion to stress, however, that the specific parameters of a WIMP candidate (mass and cross sections), which can be derived from the indirect searches, critically depend on several assumptions used in the calculations such as the estimation of the background, the halo model, the amount of WIMP in the galactic dark halo, the annihilation channels, the transport of charged particle to the Earth, etc.; thus, they have the same relative meaning as those obtained in the quest for a candidate in direct search approach as previously described.

### *5.1.3.3 Conclusions*

In conclusion, no model independent comparison with the DAMA/NaI effect is available. Only few model dependent approaches have been used in direct searches to claim for a particular model dependent comparison, which appears in addition – as mentioned above – neither based on solid procedures nor fully correct nor complete. On the other hand, the indirect search approaches, which can also offer only model dependent comparisons, are not in contradiction or in substantial agreement with the DAMA/NaI observed effect.

Thus, the interest in the further available DAMA/NaI data is increased and the analysis of the cumulative data of the seven annual cycles will be released in near future.

## **6. The new DAMA/LIBRA set-up**

After the completion of the data taking of the DAMA/NaI set-up, the procedures to install the new LIBRA set-up have been carried out. In particular, improvements have been realized in the experimental site, in the Cu box, in the shield and in the available detectors.

The LIBRA set-up consisting of  $\simeq 250$  kg of radiopure NaI(Tl) is made of 25 detectors, 9.70 kg each one. The new detectors have been realized thanks to a second generation R&D with Crismatec company, by exploiting in particular new radiopurification techniques of the NaI and TlI powders. In the framework of this R&D new materials have also been selected, prototypes have been built and tested and a devoted protocol has been fixed.

The full dismantling of the  $\simeq 100$  kg NaI(Tl) set-up, the improvements mentioned

above and the installation of all the detectors including a new PMTs' shield have been completed at end 2002. All the related procedures have been performed in HP Nitrogen atmosphere by using special masks connected to air bottles to avoid that the inner part of the Cu box, the detectors, the new PMTs' shield, etc. would be in contact with environmental air, that is to reduce at most possible surfaces' contamination by environmental Radon. Some pictures taken during the installation of the LIBRA detectors are shown in Fig. 11. Before this installation, all the Cu parts have been chemically etched following a devoted protocol and maintained in HP Nitrogen atmosphere until the installation.



Figure 11: Left picture: during the detectors installation in HP Nitrogen atmosphere. Right picture: view at end of the detectors installation. All the used materials have been deeply selected for radiopurity (see for example the cables with teflon envelop).

LIBRA will offer a relevant competitiveness e.g. because of its: i) high sensitivity; ii) standard and well defined operating procedures; iii) well known technology; iv) proved possibility of an effective control of the experimental conditions during several years of running; v) high duty cycle; vi) possibility to deeply investigate the WIMP model independent signature; vii) sensitivity to both SI and SD couplings; viii) favoured sensitivity in some of the possible particle and astrophysical models; ix) high benefits/cost.

The main aim of this new LIBRA set-up is to further investigate the WIMP component in the galactic halo with increased sensitivity thanks to the larger exposed mass and to the higher overall radiopurity. Moreover, when applicable, it offers also pulse shape discrimination capability and the possibility to achieve competitive results in the searches for other rare processes. For example, it would reach in a relatively short time a sensitivity of  $\simeq 3 \times 10^{27}$  y for possible Pauli-exclusion-principle violating processes, a sensitivity of  $\simeq 10^{24} - 10^{25}$  y for possible charge-non-conserving processes in  $^{23}\text{Na}$  and in  $^{127}\text{I}$  (depending on the counting rate in the energy region of interest), a sensitivity of  $\simeq 10^{27}$  y for the nucleon and di-nucleon decay into invisible channels, a sensitivity of  $\simeq 10^{-10} \text{ GeV}^{-1}$  on the axion-photon coupling constant from the investigation of solar axions; in addition, it could explore mass for exotic Dark

Matter candidates, such as e.g. the SIMPs, up to  $\simeq 10^{17}$  GeV and neutral nuclearites flux of  $\simeq 5 \times 10^{-12} \text{ s}^{-1}\text{cm}^{-2}\text{sr}^{-1}$ .

## 7. Conclusion

In this paper recent results achieved by the DAMA experiment at the Gran Sasso National Laboratory of I.N.F.N. have been summarized. In particular, DAMA/NaI has been a pioneer experiment running at LNGS for several years and investigating as first the WIMP annual modulation signature with suitable sensitivity and control of the running parameters. It has pointed out the presence of a modulation satisfying the several peculiarities of a WIMP induced effect and the absence of any possible systematic effects or side reactions able to mimic it, reaching a significant model independent evidence. As a corollary result, it has also pointed out the complexity of the quest for a WIMP candidate because e.g. of the present poor knowledge on the many astrophysical, nuclear and particle physics aspects and on its nature.

After the completion of the data taking of the  $\simeq 100$  kg NaI(Tl) set-up (on July 2002; full statistics of 107731 kg · d in progress to be released), as a result of the continuous efforts toward the creation of ultimate radiopure set-ups, the new DAMA/LIBRA has been realized and installed. Further R&D efforts for ultimate radiopurification of NaI(Tl) detectors are also starting again.

## 8. References

- 1) P. Belli et al., *Il Nuovo Cim.* **C 19** (1996) 537
- 2) P. Belli et al., *Astrop. Phys.* **5** (1996) 217
- 3) P. Belli et al., *Phys. Lett.* **B 387** (1996) 222
- 4) F.T. Avignone et al., *Nucl. Instr. & Meth.* **A 292** (1990) 337
- 5) R. Bernabei et al., *Nucl. Instr. & Meth.* **A 482** (2002) 728
- 6) R. Bernabei et al., *Phys. Lett.* **B 527** (2002) 182
- 7) R. Bernabei et al., *Phys. Lett.* **B 546** (2002) 23
- 8) R. Bernabei et al., *Phys. Lett.* **B 436** (1998) 379
- 9) R. Bernabei et al., *Eur. Phys. J.-direct* **C 11** (2001) 1
- 10) R. Bernabei et al., *New Journal of Physics* **2** (2000) 15.1
- 11) P. Belli et al., *Phys. Lett.* **B 465** (1999) 315
- 12) P. Belli et al., *Phys. Rev.* **D 61** (2000) 117301
- 13) R. Bernabei et al., *Phys. Lett.* **B 493** (2000) 12
- 14) R. Bernabei et al., *Il Nuovo Cim.* **A 110** (1997) 189
- 15) R. Bernabei et al., *Astrop. Phys.* **7** (1997) 73
- 16) P. Belli et al., *Nucl. Phys.* **B 563** (1999) 97
- 17) P. Belli et al., *Astrop. Phys.* **10** (1999) 115
- 18) R. Bernabei et al., *Nucl. Phys.* **A 705** (2002) 29
- 19) P. Belli et al., *Nucl. Instr. & Meth.* **A 498** (2003) 352
- 20) R. Bernabei et al., *Phys. Lett.* **B 424** (1998) 195
- 21) R. Bernabei et al., *Il Nuovo Cim.* **A 112** (1999) 545

- 22) R. Bernabei et al., *Phys. Lett. B* **450** (1999) 448
- 23) P. Belli et al., *Phys. Rev. D* **61** (1999) 023512
- 24) R. Bernabei et al., *Phys. Lett. B* **480** (2000) 23
- 25) R. Bernabei et al., *Eur. Phys. J. C* **18** (2000) 283
- 26) R. Bernabei et al., *Phys. Lett. B* **509** (2001) 197
- 27) R. Bernabei et al., *Eur. Phys. J. C* **23** (2002) 61
- 28) P. Belli et al., *Phys. Rev. D* **66** (2002) 043503
- 29) R. Bernabei et al., *Phys. Lett. B* **389** (1996) 757
- 30) R. Bernabei et al., *Il Nuovo Cimento A* **112** (1999) 1541
- 31) R. Bernabei et al., *Phys. Rev. Lett.* **83** (1999) 4918
- 32) F. Cappella et al., *Eur. Phys. J.-direct C* **14** (2002) 1
- 33) R. Bernabei et al., *Phys. Lett. B* **515** (2001) 6
- 34) R. Bernabei et al., *Phys. Lett. B* **408** (1997) 439
- 35) P. Belli et al., *Phys. Rev. C* **60** (1999) 065501
- 36) P. Belli et al., *Phys. Lett. B* **460** (1999) 236
- 37) P. Belli, R. Bernabei, C. Bacci, A. Incicchitti, R. Marcovaldi, D. Prospero,  
DAMA proposal to INFN Scientific Committee II, April 24<sup>th</sup> 1990
- 38) K.A. Drukier et al., *Phys. Rev. D* **33** (1986) 3495; K. Freese et al., *Phys. Rev. D* **37** (1988) 3388
- 39) CDMS collaboration, *Phys. Rev. Lett.* **84** (2000) 5699
- 40) EDELWEISS collaboration, *Phys. Lett. B* **513** (2001) 15
- 41) R. Luscher, talk given at Moriond, March 2003
- 42) A. Bottino et al., *Phys. Lett. B* **402** (1997) 113 ; *Phys. Lett. B* **423** (1998) 109 ; *Phys. Rev. D* **59** (1999) 095004 ; *Phys. Rev. D* **59** (1999) 095003 ; *Astrop. Phys.* **10** (1999) 203 ; *Astrop. Phys.* **13** (2000) 215 ; *Phys. Rev. D* **62** (2000) 056006 ; *Phys. Rev. D* **63** (2001) 125003 ; *Nucl. Phys. B* **608** (2001) 461
- 43) R.W. Arnowitt and B. Dutta, *hep-ph/0211417*; R.W. Arnowitt and P. Nath, *Phys. Rev. D* **60** (1999) 044002; E. Gabrielli et al., *Phys. Rev. D* **63** (2001) 025008; E. Accomando et al., *Nucl. Phys. B* **585** (2000) 124
- 44) D. Fargion et al., *Pis'ma Zh. Eksp. Teor. Fiz.* **68**, (*JETP Lett.* **68**, 685) (1998); *Astrop. Phys.* **12** (2000) 307
- 45) K. Hagiwara et al., *Phys. Rev. D* **66** (2002) 010001
- 46) P. Ullio et al., *JHEP* **0107** (2001) 044
- 47) D. Smith and N. Weiner, *Phys. Rev. D* **64** (2001) 043502
- 48) A. Alessandrello et al., *Nucl. Instr. & Meth. A* **409** (1998) 451
- 49) N. Smith, talk given at IDM02, York, September 2002
- 50) G.L. Kane et al., *hep-ph/0108138*
- 51) P. Picozza and A. Morselli, *astro-ph/0211286*; A. Morselli et al., *astro-ph/0211327*
- 52) A. Strong et al., *Astrophys. J.* **537** (2000) 763